

## OPEN

# Does Delayed-Time-Point Imaging Improve $^{18}\text{F}$ -FDG-PET in Patients With MALT Lymphoma?

## Observations in a Series of 13 Patients

Marius E. Mayerhoefer, MD, PhD,\* Chiara Giraudo, MD,\* Daniela Senn, BSc,\* Markus Hartenbach, MD,\* Michael Weber, PhD,\* Ivo Rausch, MSc,† Barbara Kiesewetter, MD,‡ Christian J. Herold, MD,\* Marcus Hacker, MD,\* Matthias Pones, MD,\* Ingrid Simonitsch-Klupp, MD,§ Leonhard Müllauer, MD,§ Werner Dolak, MD,|| Julius Lukas, MD,¶ and Markus Raderer, MD,‡

**Purpose:** To determine whether in patients with extranodal marginal zone B-cell lymphoma of the mucosa-associated lymphoid tissue lymphoma (MALT), delayed-time-point  $^{18}\text{F}$ -fluoro-2-deoxy-D-glucose-positron emission tomography ( $^{18}\text{F}$ -FDG-PET) performs better than standard-time-point  $^{18}\text{F}$ -FDG-PET.

**Materials and Methods:** Patients with untreated histologically verified MALT lymphoma, who were undergoing pretherapeutic  $^{18}\text{F}$ -FDG-PET/computed tomography (CT) and consecutive  $^{18}\text{F}$ -FDG-PET/magnetic resonance imaging (MRI), using a single  $^{18}\text{F}$ -FDG injection, in the course of a larger-scale prospective trial, were included. Region-based sensitivity and specificity, and patient-based sensitivity of the respective  $^{18}\text{F}$ -FDG-PET scans at time points 1 (45–60 minutes after tracer injection, TP1) and 2 (100–150 minutes after tracer injection, TP2), relative to the reference standard, were calculated. Lesion-to-liver and lesion-to-blood  $\text{SUV}_{\text{max}}$  (maximum standardized uptake values) ratios were also assessed.

**Results:**  $^{18}\text{F}$ -FDG-PET at TP1 was true positive in 15 of 23 involved regions, and  $^{18}\text{F}$ -FDG-PET at TP2 was true-positive in 20 of 23 involved regions; no false-positive regions were noted. Accordingly, region-based sensitivities and specificities were 65.2% (confidence interval [CI], 45.73%–84.67%) and 100% (CI, 100%–100%) for  $^{18}\text{F}$ -FDG-PET at TP1; and 87.0% (CI, 73.26%–100%) and 100% (CI, 100%–100%) for  $^{18}\text{F}$ -FDG-PET at TP2, respectively. FDG-PET at TP1 detected lymphoma in at least one nodal or extranodal region in 7 of 13 patients, and  $^{18}\text{F}$ -FDG-PET at TP2 in 10 of 13 patients; accordingly, patient-based sensitivity was 53.8% (CI, 26.7%–80.9%) for  $^{18}\text{F}$ -FDG-PET at TP1, and 76.9% (CI, 54.0%–99.8%) for  $^{18}\text{F}$ -FDG-PET at TP2. Lesion-to-liver and lesion-to-blood maximum standardized uptake value ratios were significantly lower at TP1 (ratios,  $1.05 \pm 0.40$  and  $1.52 \pm 0.62$ ) than at TP2 (ratios,  $1.67 \pm 0.74$  and  $2.56 \pm 1.10$ ;  $P = 0.003$  and  $P = 0.001$ ).

**Conclusions:** Delayed-time-point imaging may improve  $^{18}\text{F}$ -FDG-PET in MALT lymphoma.

**Key Words:** lymphoma,  $^{18}\text{F}$ -fluoro-2-deoxy-D-glucose, positron emission tomography, magnetic resonance imaging, computed tomography

(*Clin Nucl Med* 2016;41: 101–105)

Extranodal marginal zone B-cell lymphoma of the mucosa-associated lymphoid tissue (MALT) is one of the few lymphoma subtypes for which the International Conference on Malignant Lymphoma guidelines do not recommend  $^{18}\text{F}$ -fluoro-2-deoxy-D-glucose (FDG)-positron emission tomography (PET)/computed tomography (CT;  $^{18}\text{F}$ -FDG-PET/CT).<sup>1</sup> This is because MALT lymphoma has previously shown a variable FDG-avidity: whereas in most studies, MALT lymphoma was FDG-avid in 54% to 82% of the patients,<sup>2</sup> the largest and most recent study reported FDG avidity in only 28% of MALT lesions.<sup>3</sup>

Delayed-time-point  $^{18}\text{F}$ -FDG-PET has been reported to improve the sensitivity of  $^{18}\text{F}$ -FDG-PET for different malignancies,<sup>4</sup> including cholangiocarcinoma and lung cancer.<sup>5,6</sup> Whereas one previous study used dual-time-point  $^{18}\text{F}$ -FDG-PET in lymphoma, and observed higher standardized uptake values (SUVs) two hours after tracer injection,<sup>7</sup> delayed-time-point  $^{18}\text{F}$ -FDG-PET has not been evaluated in MALT lymphomas as yet, despite the potential implications for patient management.

It was, therefore, the goal of our study to determine whether in patients with MALT lymphoma, delayed-time-point  $^{18}\text{F}$ -FDG-PET yields the following: (1) a higher detection rate, and (2) a higher lesion-to-liver or lesion-to-blood contrast, than standard-time-point  $^{18}\text{F}$ -FDG-PET performed 45 to 60 minutes after tracer injection.

### MATERIALS AND METHODS

The present study was part of a prospective, institutional review board-approved trial that compared PET/CT and PET/magnetic resonance imaging (PET/MR), in oncologic patients who were referred to the local tertiary care center for staging and follow-up. Patients who gave written informed consent underwent  $^{18}\text{F}$ -FDG-PET/CT, and, directly after it,  $^{18}\text{F}$ -FDG-PET/MR, using a single tracer injection.

For the present study, only patients with previously untreated MALT lymphoma, as verified by a reference pathologist who analyzed tissue samples obtained by biopsy or surgery, according to the World Health Organization classification of hematological and lymphoid malignancies, were included. Pregnancy, general contraindications to MRI (eg, implantable medical devices, claustrophobia), elevated glucose levels ( $>150$  mg/dL), and known adverse reactions to ionized contrast media, comprised the exclusion criteria.

### Imaging Protocols

First,  $^{18}\text{F}$ -FDG-PET/CT was performed from the vertex to the upper thigh (head-first, in craniocaudal direction), using a 64-row

Received for publication July 6, 2015; revision accepted August 15, 2015.

From the \*Department of Biomedical Imaging and Image-guided Therapy, †Centre for Medical Physics and Biomedical Engineering, ‡Department of Internal Medicine I, §Institute of Pathology, ||Department of Internal Medicine III, and ¶Department of Ophthalmology and Optometry, Medical University of Vienna, Vienna, Austria.

Conflicts of interest and sources of funding: Supported by the Austrian Science Fund (FWF), project number KLIF 382. None of the authors has a conflict of interest with regard to the study or its results.

Correspondence to: Marius E. Mayerhoefer, MD, PhD, Department of Biomedical Imaging and Image-guided Therapy, Medical University of Vienna, Waehringer Guertel 18-20, 1090 Vienna, Austria.  
E-mail: marius.mayerhoefer@meduniwien.ac.at.

Copyright © 2015 Wolters Kluwer Health, Inc. All rights reserved. This is an open-access article distributed under the terms of the Creative Commons Attribution-Non Commercial-No Derivatives License 4.0 (CCBY-NC-ND), where it is permissible to download and share the work provided it is properly cited. The work cannot be changed in any way or used commercially.

ISSN: 0363-9762/16/4102-0101

DOI: 10.1097/RLU.0000000000001005

multidetector hybrid system (Biograph TruePoint 64; Siemens, Erlangen, Germany), with an axial field of view (FOV) of 216 mm and a PET sensitivity of 7.6 counts per second/kBq. Patients fasted for 5 hours before imaging. Positron emission tomography (PET) was performed 45 to 60 minutes after an intravenous administration of 300 MBq of  $^{18}\text{F}$ -FDG (time point 1 [TP1]), with 3-minute-per-bed position, 4 iterations, and 21 subsets, a 5-mm slice thickness, and a  $168 \times 168$  matrix, using the point-spread-function (PSF)-based reconstruction algorithm TrueX. Computed tomographic maps were used for attenuation correction. Venous-phase contrast-enhanced CT was obtained after the intravenous injection of 100 mL of a tri-iodinated, nonionic contrast medium at a rate of 2 mL/s; a tube voltage of 120 kV, a tube current of 230 mA, a collimation of  $64 \times 0.6$  mm, a 3-mm slice thickness at a 2-mm increment, and a  $512 \times 512$  matrix.

Directly after the PET/CT,  $^{18}\text{F}$ -FDG-PET/MR was performed, covering the same anatomy (head first, in craniocaudal direction), and using a fully integrated 3-T system (Biograph mMR; Siemens, Erlangen, Germany) with high-performance gradient systems (45 mT/m), a slew rate of 200 T/m per second, and equipped with a phased-array body coil. The system offers an axial field of view (FOV) of 258 mm, and a sensitivity of 13.2 counts per second/kBq, for PET.  $^{18}\text{F}$ -FDG-PET was performed 100–150 minutes after the original, intravenous tracer administration (time point 2, TP2), with 5-minute per bed position, 3 iterations, and 21 subsets, a 4.2-mm slice thickness, and a  $172 \times 172$  matrix, using the PSF-based reconstruction algorithm HD-PET. Two axial, two-point, Dixon, 3-dimensional, volume-interpolated T1-weighted breath-hold MR sequences were acquired for attenuation correction (AC), and for anatomic correlation, using the following parameters: repetition time (TR)/echo times (TE), 4.02 (AC, 3.6) ms/1.23, 2.46 ms; one average, two echoes; flip angle, 10 degrees; matrix,  $320 \times 175$  (AC,  $192 \times 79$ ); FOV,  $430 \times 309$  (AC,  $328 \times 500$ ) mm; and slice thickness, 3 mm with a 0.6-mm gap. A single-shot, echoplanar imaging (EPI)-based, spectral adiabatic inversion recovery diffusion-weighted imaging (DWI) sequence was obtained with the following parameters: *b* values, 50 and 800; TR/TE, 6800/63 ms; 6 averages and one echo; flip angle, 180 degrees; matrix,  $168 \times 104$ ; FOV,  $440 \times 340$  mm; slice thickness, 6-mm, with a 1.2-mm gap.

No diuretic or spasmolytic medications for improved evaluation of the urinary tract/bladder or gastrointestinal tract were administered before PET/CT or PET/MR.

### Lymphoma Detectability

A board-certified nuclear medicine physician and a board-certified radiologist rated all images in consensus. The 14 nodal regions defined at the Rye symposium (right/left cervical; right/left axillary; right/left infraclavicular; mediastinal; hilar; mesenteric; para-aortic; right/left pelvic; and right/left inguinal),<sup>8</sup> and 12 extranodal regions were evaluated: Waldeyer ring; lungs; liver; spleen; stomach; small intestine; large intestine; right and left kidney; bones; soft tissues (skin/fat/muscle); and other organs/tissues (e.g., lacrimal glands). On both the  $^{18}\text{F}$ -FDG-PET of the PET/CT at TP1, and the  $^{18}\text{F}$ -FDG-PET of the PET/MR at TP2 (which was evaluated separately, and blinded to the TP1 results), nodal and extranodal regions were rated as involved when there was at least one focal (or, for bone marrow, also diffuse) area of increased tracer accumulation relative to the surrounding tissue. The spleen was rated as positive if nodular or diffuse tracer uptake higher than that in the liver was observed.

### Lesion-to-Liver and Lesion-to-Blood Contrast

After the independent lesion assessment at TP1 and TP2, quantitative analysis was performed, this time with access to

histology and DWI. Maximum and mean SUVs ( $\text{SUV}_{\text{max}}$ ,  $\text{SUV}_{\text{mean}}$ ) on  $^{18}\text{F}$ -FDG-PET were measured for up to 3 largest, previously identified lymphoma manifestations of each patient at TP1 and TP2 based on isocontour volumes of interest (VOIs) that included all voxels greater than 50% of the  $\text{SUV}_{\text{max}}$  of each lesion. For a lesion that was only visible on  $^{18}\text{F}$ -FDG-PET at one time point, the VOI was copied from the PET that visualized the lesion to the other PET. For lymphoma lesions that were not visible on  $^{18}\text{F}$ -FDG-PET at either time point but were visible on DWI, which has high sensitivity for MALT lymphoma,<sup>9</sup> lesion contours were defined manually on DWI, provided that the lesion(s) had been confirmed by histology.  $\text{SUV}_{\text{max}}$  and  $\text{SUV}_{\text{mean}}$  were also measured in the lesion-free liver parenchyma and the mediastinal blood pool (ie, aortic arch), using spherical VOIs with diameters of 3 cm (liver) and 1.5 cm (blood pool).

### Statistical Analysis

Histology was the basis for the reference standard and was required for all extranodal lymphoma manifestations. For suspected lymph node involvement, histological verification in at least a single nodal region was required; in case of involvement of multiple nodal regions, positive  $^{18}\text{F}$ -FDG-PET findings at both time points, or a positive DWI finding in addition to a positive  $^{18}\text{F}$ -FDG-PET finding at one time point, was required to verify each nonhistologically proven region. Similarly, for verification of uninvolved (ie, disease-free) regions, agreement of  $^{18}\text{F}$ -FDG-PET at both time points, or agreement of  $^{18}\text{F}$ -FDG-PET at one time point with DWI, was used as the reference standard. This strategy was chosen because it was regarded as clinically infeasible, as well as unethical, to verify regions that are negative at imaging by biopsy/histology.

Region-based sensitivity and specificity as well as patient-based sensitivity (but not specificity because only patients with histologically proven MALT lymphoma in at least one region were included in this study), as well as their respective 95% confidence intervals (CI), were calculated for  $^{18}\text{F}$ -FDG-PET at TP1, and for  $^{18}\text{F}$ -FDG-PET at TP2. Patient-based lesion-to-liver and lesion-to-blood ratios of  $\text{SUV}_{\text{max}}$  and  $\text{SUV}_{\text{mean}}$  values were calculated separately at TP1 and TP2 and were compared using paired *t* tests (using arithmetic means in patients with >1 lesion). The specified level of significance was  $P \leq 0.05$ .

## RESULTS

Thirteen patients (eight women and 5 men; mean age,  $66.8 \pm 14.3$  years) with 23 lymphoma manifestations met our criteria for participation in the study (Table 1). All 21 histologically proven lymphoma manifestations underwent biopsy before the  $^{18}\text{F}$ -FDG-PET/CT and -PET/MR examinations. Owing to work-flow reasons,  $^{18}\text{F}$ -FDG-PET/MR was performed before  $^{18}\text{F}$ -FDG-PET/CT in one patient, and thus, PET/MR was considered as  $^{18}\text{F}$ -FDG-PET at TP1, and PET/CT as  $^{18}\text{F}$ -FDG-PET at TP2 in this case. The mean time interval after the  $^{18}\text{F}$ -FDG injection was  $54.5 \pm 6.0$  minutes for TP1 and  $120.3 \pm 11.1$  minute for TP2.

$^{18}\text{F}$ -FDG-PET at TP1 was true positive (ie, agreed with the reference standard) in 15 of 23 involved regions, and  $^{18}\text{F}$ -FDG-PET at TP2 was true positive in 20 of 23 involved regions (Table 1, Figs. 1 and 2). Since there were no false-positive results at either time point, region-based sensitivities and specificities were 65.2% (CI, 45.73%–84.67%) and 100% (CI, 100%–100%) for  $^{18}\text{F}$ -FDG-PET at TP1, and 87.0% (CI, 73.26%–100%) and 100% (CI, 100%–100%) for  $^{18}\text{F}$ -FDG-PET at TP2, respectively. Accordingly,  $^{18}\text{F}$ -FDG-PET at TP1 detected lymphoma in at least one nodal or extranodal region in 7 of 13 patients, and  $^{18}\text{F}$ -FDG-PET at TP2 in 10 of 13 patients, relative to the reference standard. Thus, patient-based sensitivity was 53.8% (CI, 26.7%–80.9%) for  $^{18}\text{F}$ -FDG-PET at TP1, and 76.9% (CI, 54.0%–99.8%) for  $^{18}\text{F}$ -FDG-PET at TP2.

**TABLE 1.** Distribution of MALT Lymphoma Manifestations, and <sup>18</sup>F-FDG-PET-Positivity at Time Point 1 (TP1, 45-60 minutes After Tracer Injection) and Time Point 2 (TP2, 100-150 min After Tracer Injection)

Anatomic Region	PET-Positive at TP1	PET-Positive at TP2	Reference Standard	Reference Type
Cervical lymph nodes	3	3	3	Histology
Mesenteric lymph nodes	1	1	1	DWI + PET*
Waldeyer ring	1	1	1	DWI + PET*
Lungs	3	3	3	Histology
Stomach	2	4	4	Histology
Small bowel	0	0	2	Histology
Liver	0	2	2	Histology
Kidneys	1	2	2	Histology
Bone	1	1	1	Histology
Others—breast	1	1	1	Histology
Others—lacrimal gland	1	1	1	Histology
Others—parotid gland	1	1	1	Histology
Others—urinary bladder	0	0	1	Histology
Total	15	20	23	—

\*Agreement of <sup>18</sup>F-FDG-PET at both time points or a positive DWI finding in addition to a positive <sup>18</sup>F-FDG-PET finding at one time point (TP1, TP2).

With regard to lesion-to-liver and lesion-to-blood SUV<sub>max</sub> ratios, significant differences were observed between <sup>18</sup>F-FDG-PET at TP1 (ratios, 1.05 ± 0.40 and 1.52 ± 0.62) and <sup>18</sup>F-FDG-PET at TP2 (ratios, 1.67 ± 0.74 and 2.56 ± 1.10) (*P* = 0.003 and *P* = 0.001). The lesion-to-blood, and lesion-to-liver SUV<sub>mean</sub> ratios also differed significantly between <sup>18</sup>F-FDG-PET at TP1 (ratios, 1.11 ± 0.40 and 1.38 ± 0.54) and <sup>18</sup>F-FDG-PET at TP2 (ratios, 1.77 ± 1.22 and 2.32 ± 1.26) (*P* = .035 and *P* = 0.006).

**DISCUSSION**

Our observations suggest that in untreated MALT lymphoma, the performance of <sup>18</sup>F-FDG-PET may indeed improve when PET is performed after an extended time interval, ie, approximately 2 hours

after radiotracer injection. Notably, 3 of 13 patients, which were (completely) false negative on PET at TP1 (the standard time point), were true positive at TP2 (ie, the delayed time point; Figs. 1 and 2).

Lesion-to-liver as well as lesion-to-blood contrast of MALT lymphomas on <sup>18</sup>F-FDG-PET was significantly higher at TP2 than at TP1, regardless of whether SUV<sub>max</sub> or SUV<sub>mean</sub> were used. This seems plausible because several malignant tumors show a prolonged uptake of FDG, with higher SUV<sub>max</sub> values on delayed <sup>18</sup>F-FDG-PET<sup>4,6</sup>; in addition, the high glucose-6-phosphatase activity of the liver leads to an early peak followed by a decrease in intracellular FDG retention, and the blood pool clearance of <sup>18</sup>F-FDG increases over time.<sup>4,10</sup> A combination of these factors is the most likely explanation for our own findings.

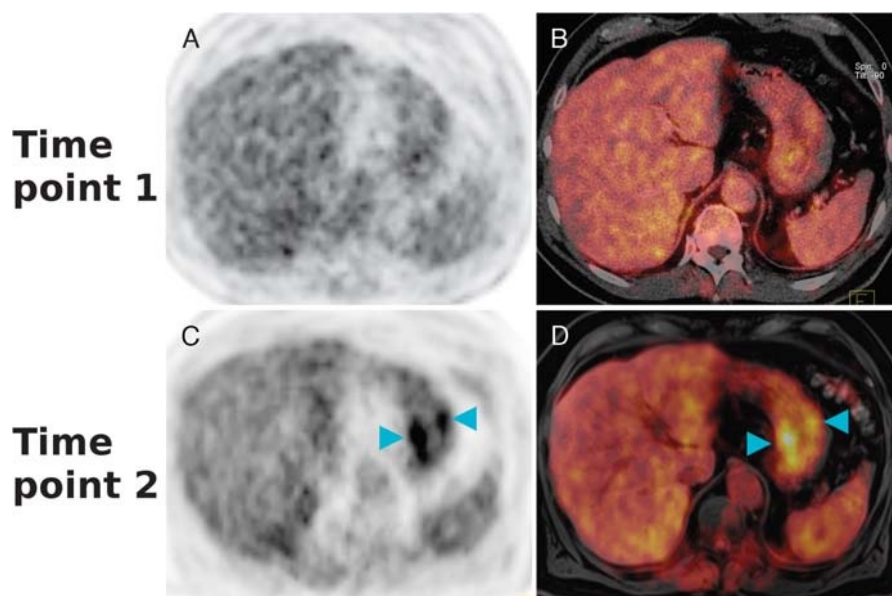


**FIGURE 1.** A 70-year-old man with a histologically verified MALT lymphoma of the stomach. On the <sup>18</sup>F-FDG-PET (A) and the corresponding color-coded fused <sup>18</sup>F-FDG-PET/CT (B) at time point 1 (ie, 49 minutes after tracer injection), no increased tracer uptake is visible. The <sup>18</sup>F-FDG-PET (C) and the fused color-coded <sup>18</sup>F-FDG-PET/MR (D) at time point 2 (ie, 111 minutes after tracer injection), however, clearly show the extranodal lymphoma involvement with an increased tracer uptake in the stomach wall (light-blue arrowheads).

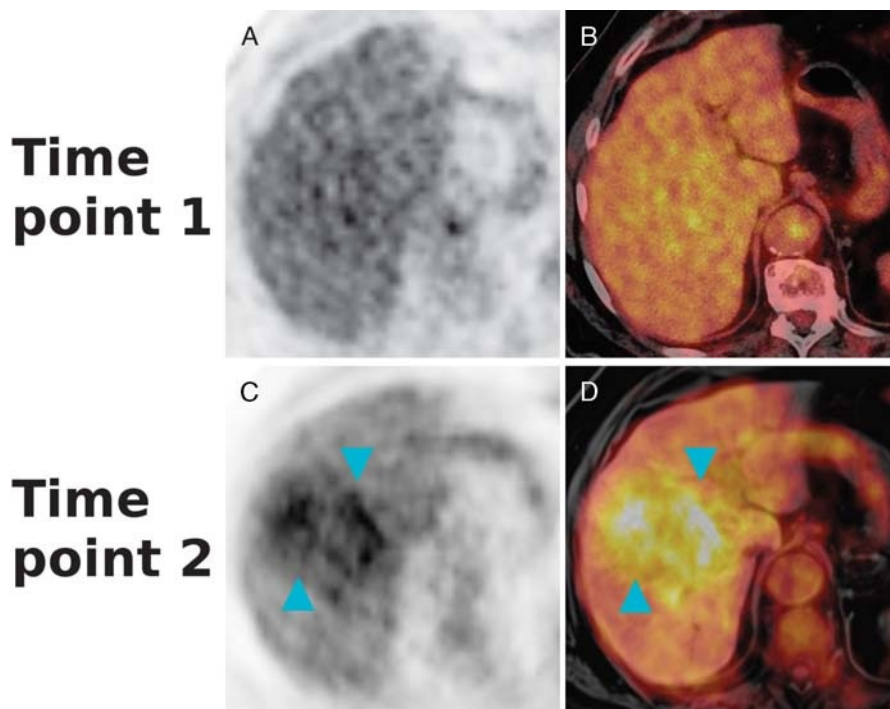


**FIGURE 2.** An 85-year-old man with a histologically verified MALT lymphoma in the right liver lobe. On the  $^{18}\text{F}$ -FDG-PET (A) and the corresponding color-coded fused  $^{18}\text{F}$ -FDG-PET/CT (B) at time point 1 (ie, 52 minutes after tracer injection), no clear, focal, increased tracer uptake is visible. The  $^{18}\text{F}$ -FDG-PET (C) and the fused color-coded  $^{18}\text{F}$ -FDG-PET/MR (D) performed at time point 2 (ie, 112 minutes after tracer injection), however, clearly show the large extranodal lymphoma manifestation with an increased tracer uptake (light-blue arrowheads) relative to the surrounding liver parenchyma.

Notably, dual-time-point imaging, or even delayed-time-point imaging, may be problematic for  $^{18}\text{F}$ -FDG-PET/CT owing to workflow and patient throughput considerations. For  $^{18}\text{F}$ -FDG-PET/MR, however, this would not be problematic because patients spend approximately 1 hour in the scanner for a whole-body examination, thus enabling PET image acquisition at standard and delayed time points. Thus, for patients with MALT lymphoma, the use of PET/MR, instead of PET/CT, may be justifiable.

The importance of  $^{18}\text{F}$ -FDG-PET for lymphoma, in general, and thus also for MALT lymphoma, lies in its ability to quantitatively assess disease at the cellular level, which no other imaging technique can presently provide. Although DWI, which visualizes cell density, is being discussed as a possible alternative for lymphoma staging/restaging, it cannot assess changes in metabolism, is prone to artifacts,<sup>9</sup> and apparent diffusion coefficients are sensitive to the choice of acquisition technique (ie, breath-holding, respiratory triggering, or free-breathing) and fat suppression technique.<sup>11,12</sup>

Our use of 2 different devices (a PET/CT and a PET/MR system) at the 2 time points may be considered a limitation to our study because attenuation correction techniques for  $^{18}\text{F}$ -FDG-PET differ between the 2 techniques. However, previous studies (which used the same PET/MR system as in our study) have shown that lesion visualization on  $^{18}\text{F}$ -FDG-PET is not negatively affected in PET/MR compared to PET/CT.<sup>13–16</sup> Mean SUV and SUV<sub>max</sub> values in these studies either did not differ significantly between  $^{18}\text{F}$ -FDG-PET/CT and  $^{18}\text{F}$ -FDG-PET/MR<sup>13,14</sup> or they were significantly lower on  $^{18}\text{F}$ -FDG-PET/MR.<sup>15,16</sup> Thus, it seems highly unlikely that the improved lesion detectability on delayed-time-point  $^{18}\text{F}$ -FDG-PET in our study was caused by the difference in PET acquisition/attenuation correction techniques. Moreover, lesion-to-liver and lesion-to-blood SUV ratios, rather than absolute SUVs, were used for all quantitative comparisons, and, in the single patient

who underwent  $^{18}\text{F}$ -FDG-PET/MR before  $^{18}\text{F}$ -FDG-PET/CT, the same trend was observed as in all other patients: a higher lesion-to-liver and lesion-to-blood contrast on delayed-time-point  $^{18}\text{F}$ -FDG-PET. Another limitation refers to the fact that we did not administer diuretic or spasmolytic medications before imaging because this strategy is not used routinely in our institution. Nevertheless, use of these medications might possibly have enabled/improved the detection of lymphoma manifestations in the urinary and gastrointestinal tract; after all, 2 lesions in the small bowel and one lesion in the urinary bladder were missed at both  $^{18}\text{F}$ -FDG-PET time points.

In conclusion, the observations in our small series of patients with MALT lymphoma indicate that delayed-time-point  $^{18}\text{F}$ -FDG-PET may possibly provide better lesion detectability and higher lesion-to-liver and lesion-to-blood contrast, than standard-time-point  $^{18}\text{F}$ -FDG-PET. Further studies with larger cohorts that also collect data at multiple time points—even beyond 2 hours after tracer injection—using a single device (PET/CT or PET/MR) are required to confirm our findings and thus determine whether  $^{18}\text{F}$ -FDG-PET may have a role in the workup of patients with MALT lymphoma after all.

## REFERENCES

- Cheson BD, Fisher RI, Barrington SF, et al. Recommendations for initial evaluation, staging, and response assessment of Hodgkin and non-Hodgkin lymphoma: the Lugano classification. *J Clin Oncol*. 2014;32:3059–3068.
- Weiler-Sagie M, Bushelev O, Epelbaum R, et al. (18)F-FDG avidity in lymphoma readdressed: a study of 766 patients. *J Nucl Med*. 2010;51:25–30.
- Park SH, Lee JJ, Kim HO, et al. (18)F-Fluorodeoxyglucose (FDG)-positron emission tomography/computed tomography in mucosa-associated lymphoid tissue lymphoma: variation in (18)F-FDG avidity according to site involvement. *Leuk Lymphoma*. 2015;25:1–18.

4. Cheng G, Torigian DA, Zhuang H, et al. When should we recommend use of dual time-point and delayed time-point imaging techniques in FDG PET? *Eur J Nucl Med Mol Imaging*. 2013;40:779–787.
5. Choi EK, Yoo IeR, Kim SH, et al. The clinical value of dual-time point 18 F-FDG PET/CT for differentiating extrahepatic cholangiocarcinoma from benign disease. *Clin Nucl Med*. 2013;38:e106–e111.
6. Cheng G, Alavi A, Werner TJ, et al. Serial changes of FDG uptake and diagnosis of suspected lung malignancy: a lesion-based analysis. *Clin Nucl Med*. 2014;39:147–155.
7. Shinya T, Fujii S, Asakura S, et al. Dual-time-point F-18 FDG PET/CT for evaluation in patients with malignant lymphoma. *Ann Nucl Med*. 2012;26:616–621.
8. Armitage JO. Staging non-Hodgkin lymphoma. *CA Cancer J Clin*. 2005;55:368–376.
9. Mayerhoefer ME, Karanikas G, Kletter K, et al. Evaluation of diffusion-weighted MRI for pretherapeutic assessment and staging of lymphoma: results of a prospective study in 140 patients. *Clin Cancer Res*. 2014;20:2984–2993.
10. Chirindel A, Alluri KC, Tahari AK, et al. Liver standardized uptake value corrected for lean body mass at FDG PET/CT: effect of FDG uptake time. *Clin Nucl Med*. 2015;40:e17–e22.
11. Larsen NE, Haack S, Larsen LP, et al. Quantitative liver ADC measurements using diffusion-weighted MRI at 3 Tesla: evaluation of reproducibility and perfusion dependence using different techniques for respiratory compensation. *MAGMA*. 2013;26:431–442.
12. Mürtz P, Tsesarskiy M, Kowal A, et al. Diffusion-weighted magnetic resonance imaging of breast lesions: the influence of different fat-suppression techniques on quantitative measurements and their reproducibility. *Eur Radiol*. 2014;24:2540–2551.
13. Rauscher I, Eiber M, Fürst S, et al. PET/MR imaging in the detection and characterization of pulmonary lesions: technical and diagnostic evaluation in comparison to PET/CT. *J Nucl Med*. 2014;55:724–729.
14. Heusch P, Buchbender C, Köhler J, et al. Thoracic staging in lung cancer: prospective comparison of 18 F-FDG PET/MR imaging and 18 F-FDG PET/CT. *J Nucl Med*. 2014;55:373–378.
15. Eiber M, Takei T, Souvatzoglou M, et al. Performance of whole-body integrated 18 F-FDG PET/MR in comparison to PET/CT for evaluation of malignant bone lesions. *J Nucl Med*. 2014;55:191–197.
16. Jeong JH, Cho IH, Kong EJ, et al. Evaluation of Dixon sequence on hybrid PET/MR compared with contrast-enhanced PET/CT for PET-positive lesions. *Nucl Med Mol Imaging*. 2014;48:26–32.